



1 **Probabilistic characteristics of narrow-band long wave run-up onshore**

2

3

Sergey Gurbatov¹⁾ and Efim Pelinovsky^{2,3)}

4 1) National Research University – Lobachevsky State University, Nizhny Novgorod, Russia

5 2) National Research University – Higher School of Economics, Moscow, Russia

6 3) Institute of Applied Physics, Nizhny Novgorod, Russia

7

8 **Abstract**

9 The run-up of random long wave ensemble (swell, storm surge and tsunami) on the constant-
10 slope beach is studied in the framework of the nonlinear shallow-water theory in the
11 approximation of non-breaking waves. If the incident wave approaches the shore from deepest
12 water, runup characteristics can be found in two stages: at the first stage, linear equations are
13 solved and the wave characteristics at the fixed (undisturbed) shoreline are found, and, at the
14 second stage, the nonlinear dynamics of the moving shoreline is studied by means of the
15 Riemann (nonlinear) transformation of linear solutions. In the paper, detail results are obtained
16 for quasi-harmonic (narrow-band) waves with random amplitude and phase. It is shown that the
17 probabilistic characteristics of the runup extremes can be found from the linear theory, while the
18 same ones of the moving shoreline - from the nonlinear theory. The role of wave breaking due to
19 large-amplitude outliers is discussed, so that it becomes necessary to consider wave ensembles
20 with non-Gaussian statistics within the framework of the analytical theory of non-breaking
21 waves. The basic formulas for calculating the probabilistic characteristics of the moving
22 shoreline and its velocity through the incident wave characteristics are given. They can be used
23 for estimates of the flooding zone characteristics in marine natural hazards.

24

25 **Keywords:** tsunami, storm surge, long wave runup, Carrier-Greenspan transform, statistical
26 characteristics

27

28 **1. Introduction**

29 The flooded area size, the water flow depth and its speed on the coast, the coastal topography
30 characteristics and the features of the coastal zone development determine the consequences of
31 marine natural disasters on the coast. The catastrophic events of recent years are well known,
32 when tsunami waves and storm surges caused significant damage on the coast and people's
33 death. It is worth saying that only in 2018 two catastrophic tsunamis occurred in Indonesia,
34 leading to the death of several thousand people (on Sulawesi Island in September and in the
35 Sunda Strait in December). The calculations of the coast flooding in tsunamis and storm surges
36 is mainly carried out within the framework of nonlinear shallow-water equations, taking into
37 account the variable roughness coefficient for various areas of the coastal zone (Kaiser et al,



38 2011; Choi et al, 2012). The characteristics of the coastal destruction is determined either by
39 using fragility curves (Macabuag et al, 2016; Park et al, 2017) or by using a direct calculation of
40 the tsunami forces (Qi et al, 2014; Ozer et al, 2015a, b; Kian et al, 2016; Xiong et al., 2019).

41 The computation accuracy was tested on a series of benchmarks, including the idealized
42 problem of the wave run-up onto the impenetrable slope of a constant gradient without friction
43 (Synolakis et al, 2008). The nonlinear shallow water equations for the bottom geometry of this
44 kind are linearized by using the hodograph (Legendre) transformations. This step makes it
45 possible to obtain a number of exact solutions describing the run-up on the coast. This approach,
46 first suggested in (Carrier and Greenspan, 1958), was later on used to analyze the run-up of
47 single and periodic waves of various shapes (Synolakis, 1987; Pelinovsky and Mazova, 1992;
48 Tinti and Toniti, 2005; Madsen and Fuhrman, 2008; Madsen and Schaffer, 2010; Antuano and
49 Brocchini, 2008, 2010; Didenkulova, 2009; Dobrokhotov et al, 2015; Aydin and Kanoglu, 2017).
50 Moreover, such approach made it possible to determine the conditions for the wave breaking.
51 The latter means the presence of steep fronts (gradient catastrophe) within the hyperbolic
52 shallow water equation framework. The Carrier-Greenspan transformation was further
53 generalized for the case of waves in an inclined channel of an arbitrary variable cross section
54 (Rybkin et al, 2013; Pedersen, 2016; Shimozone, 2016; Anderson et al, 2017; Raz et al, 2018). In
55 a number of practical cases, its use proves to be more efficient than the direct numerical
56 computation within the 2D shallow water equation framework (Harris et al, 2015, 2016).

57 Due to bathymetry variability and shoreline complexity, diffraction and scattering effects
58 lead to an irregular shape of the waves approaching the coast. Moreover, very often not the
59 leading wave turns out to be the maximum one. Such typical tsunami wave records on tide-
60 gauges are well known and are not shown here. It is applied even more to swell waves, which in
61 some cases approach the coast without breaking (Huntley et al, 1977; Hughes et al, 2010). As a
62 result, statistical wave theory can be applied to such records and with their help, nonlinear
63 shallow water equations in the random function class can be solved. This approach was used to
64 describe the statistical moments of the long wave run-up characteristics in (Didenkulova et al,
65 2008, 2010, 2011). Special laboratory experiments were also conducted on irregular wave run-up
66 on a flat slope, the results of which are not very well described by theoretical dependencies
67 (Denissenko et al, 2011, 2013). As for field data, we are acquainted with two papers: (Huntley et
68 al, 1977; Hughes et al, 2010), where the statistical characteristics of the moving shoreline on two
69 Canadian and one Australian beaches were calculated. They confirmed the fact that the wave
70 process on the coast is not Gaussian. In our opinion, the main problem in the theoretical model of
71 describing the irregular wave run-up on the shore is associated with the use of two hypotheses: 1)



72 the small amplitude wave field (in the linear problem) is Gaussian; 2) waves run-up on the shore
73 without breaking. It is obvious, however, that in the nonlinear wave field some broken waves can
74 always be present. They affect the distribution function tails and, thus, the statistical moments of
75 the run-up characteristics as well.

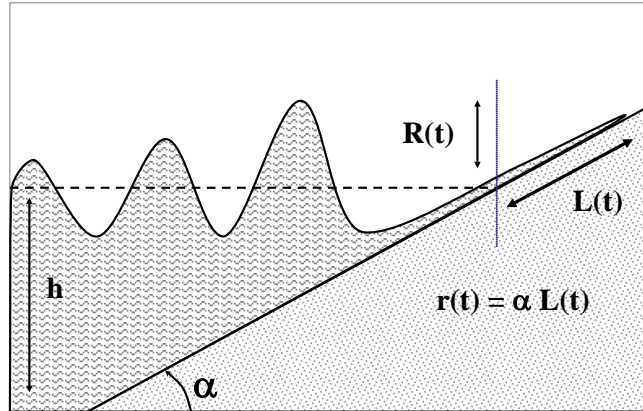
76 The connection of the run-up parameters at the nonlinear stage with the linear field at a
77 fixed point is described either in a parametric form or implicitly in a nonlinear equation
78 (Didenkulova et al. 2010). This does not allow using the standard methods of random processes.
79 At the same time, it is known that this implicit equation is equivalent to a partial first-order
80 differential equation (PDE), that is, to the simple or Riemann wave equation (Rudenko and
81 Soluyan, 1977). In statistical problems, this equation arises in nonlinear acoustics. This equation
82 or its generalization, the nonlinear diffusion equation called the Burgers equation (Burgers et al,
83 1974) is the model equation in the hydrodynamic turbulence theory (Frisch, 1995). It should be
84 noted that for the one-dimensional Burgers turbulence, as well as its three-dimensional version,
85 used for the model description of the large-scale Universe structure (Gurbatov et al, 2012). It is
86 possible to give an almost comprehensive statistical description for certain initial conditions
87 (Gurbatov et al, 1991, 1997, 2011; Gurbatov and Saichev, 1993; Molchanov et al, 1995; Frisch,
88 1995; Woyczynski, 1998; Frisch and Bec, 2001; Bec and Khanin, 2007). In particular, single-
89 point and two-point probability distributions of the velocity field and even N -point probability
90 distributions and, accordingly, multi-point moment functions were found. This partially allows
91 using a mathematical approach developed in statistical nonlinear acoustics. An experimental
92 study of the nonlinear evolution of random quasi-monochromatic waves and the probability
93 distributions and spectra analysis have been carried out in acoustics more than once. They
94 confirmed theoretical conclusions; see, for example (Gurbatov et al, 2018, 2019).

95 This paper is devoted to the analytical study of the probabilistic characteristics of the long
96 narrow-band wave run-up on the coast. Section 2 gives the basic equations of nonlinear shallow
97 water theory and the Carrier-Greenspan transformation, with the latter making it possible to
98 linearize the nonlinear equations. Section 3 describes the moving shoreline dynamics when the
99 deterministic sine wave climbs on the slope. The probability characteristics of the deformed sine
100 oscillations of the moving shoreline with a random phase are described in Sect. 4. Section 5
101 contains the probabilistic characteristics on the vertical displacement of the moving shoreline if
102 the incident narrow-band wave has a random amplitude and phase. The discussion of the wave
103 breaking effects and their influence on the distribution of the run-up characteristics is given in
104 Sect. 6. The results obtained are summarized in Sect. 7.

105



106 **2. Basic equations and transformations**



107
 108 Fig. 1. The problem geometry
 109

110 Here we will consider the classical formulation of the problem of a long wave run-up on the
 111 constant-gradient slope in an ideal fluid (Fig. 1). The wave is one-dimensional and propagates
 112 along the x -axis directed onshore. The basin depth is a linear depth function: $h(x) = -\alpha x$, where
 113 α is the inclination angle tangent and point $x = 0$ corresponds to a fixed unperturbed water
 114 shoreline. $L(t)$ and $r(t)$ describe horizontal and vertical displacement of the moving shoreline,
 115 and $R(t)$ is the water level oscillations at $x = 0$. The bottom and the shore are assumed
 116 impenetrable. The long wave dynamics is described by nonlinear shallow water equations:

117
$$\frac{\partial u}{\partial t} + u \frac{\partial u}{\partial x} + g \frac{\partial \eta}{\partial x} = 0, \quad (2.1)$$

118
$$\frac{\partial \eta}{\partial t} + \frac{\partial}{\partial x} [(-\alpha x + \eta)u] = 0. \quad (2.2)$$

119 Here, $\eta(x,t)$ is the free surface elevation above the undisturbed water level, and $u(x,t)$ is the
 120 depth-averaged flow velocity (within the shallow water theory, the flow velocity is the same on
 121 all horizons), and g is the gravity acceleration. Obviously, after introducing total depth

122
$$H(x,t) = -\alpha x + \eta(x,t), \quad (2.3)$$

123 equations (2.1) and (2.2) are a hyperbolic system with constant coefficients. This fact makes it
 124 possible to transform the system into a linear equation one by using a hodograph (Legendre)
 125 transformation, which was done in the pioneering work (Carrier and Greenspan, 1958). As a



126 result, the wave field is described by a linear wave equation in the ‘cylindrical’ coordinate
127 system

$$128 \quad \frac{\partial^2 \Phi}{\partial \lambda^2} - \frac{\partial^2 \Phi}{\partial \sigma^2} - \frac{1}{\sigma} \frac{\partial \Phi}{\partial \sigma} = 0, \quad (2.4)$$

129 and all variables are expressed in terms of an auxiliary wave function $\Phi(\sigma, \lambda)$ using explicit
130 formulas

$$131 \quad \eta = \frac{1}{2g} \left(\frac{\partial \Phi}{\partial \lambda} - u^2 \right), \quad (2.5)$$

$$132 \quad u = \frac{1}{\sigma} \frac{\partial \Phi}{\partial \sigma}, \quad (2.6)$$

$$133 \quad x = \frac{1}{2\alpha g} \left(\frac{\partial \Phi}{\partial \lambda} - u^2 - \frac{\sigma^2}{2} \right), \quad (2.7)$$

$$134 \quad t = \frac{1}{\alpha g} (\lambda - u). \quad (2.8)$$

135 It should be noted that the variable σ is proportional to the total water depth.

$$136 \quad \sigma = 2\sqrt{gH} = 2\sqrt{g(-\alpha x + \eta)}, \quad (2.9)$$

137 so, the wave equation (2.4) is solved on the semi-axis $\sigma \geq 0$, and this coordinate plays the radius
138 role in the cylindrical coordinate system. We would like to emphasize that the point $\sigma = 0$
139 corresponds to a moving shoreline, and therefore, the original problem, solved in the area with a
140 unknown boundary, is reduced to a fixed area problem.

141 It is important to note that the hodograph transformation is valid if the Jacobian
142 transformation is non-zero

$$143 \quad J = \frac{\partial(x, t)}{\partial(\sigma, \lambda)} \neq 0. \quad (2.10)$$

144 It is the case when a gradient catastrophe, identified in the framework of the shallow-water
145 theory with the wave breaking, does not occur. The necessary condition for the wave breaking
146 absence is the boundedness and smoothness of all solutions; this question will be discussed
147 further on.

148 We will assume that the wave approaches the coast from the area far from the shoreline (
149 $x \rightarrow -\infty$), where the wave is linear. Then it is obvious that the function $\Phi(\sigma, \lambda)$ can be
150 completely found from the linear theory. The difficulty in finding the wave field in the near-



151 shoreline area is due to the implicit transformation of the coordinates (x, t) to (σ, λ) . However,
152 for the most interesting point of the moving shoreline $\sigma = 0$ (its dynamics determines the size of
153 the flooded area on the coast) all the formulas become explicit. In particular, from (2.5) and (2.6)
154 follows

$$155 \quad r(t) = R \left[t + \frac{u(t)}{\alpha g} \right] - \frac{u(t)^2}{2g}, \quad (2.11)$$

$$156 \quad u(t) = U \left[t + \frac{u(t)}{\alpha g} \right], \quad (2.12)$$

157 where $r(t)$ and $u(t)$ are the vertical displacement of the moving shoreline and its speed, and the
158 functions $R(t)$ and $U(t)$ determine the field characteristics at the fixed point $(x = 0)$ from the
159 linear theory

$$160 \quad R(t) = \frac{1}{2g} \frac{\partial \Phi(\sigma = 0, \lambda)}{\partial \lambda} \Big|_{\lambda = \alpha g t}, \quad U(t) = \frac{1}{\sigma} \frac{\partial \Phi(\sigma, \lambda)}{\partial \sigma} \Big|_{\sigma = 0, \lambda = \alpha g t}. \quad (2.13)$$

161 Then we add the obvious kinematic relations for the vertical displacement and velocity of the last
162 sea point along the slope.

$$163 \quad u(t) = \frac{1}{\alpha} \frac{dr(t)}{dt}, \quad U(t) = \frac{1}{\alpha} \frac{dR(t)}{dt}. \quad (2.14)$$

164 Let us note that formula (2.12) is identical to the so-called Riemann wave or a simple
165 wave in a nonlinear non-dispersive medium (in particular, in nonlinear acoustics), if we consider
166 the parameter $1/\alpha g$ to be a ‘coordinate’; see, for example, (Rudenko and Soluyan, 1977,
167 Gurbatov et al, 1991, 2011). Moreover, formula (2.13) describes the integral over the Riemann
168 wave. This analogy proves to be very useful when transferring the already known results in the
169 wave nonlinear theory to the run-up characteristics described by the ODE.

170 Detailed calculations of the long wave run-up on the coast were carried out repeatedly;
171 see, for example (Carrier and Greenspan, 1958; Synolakis, 1987; Pelinovsky and Mazova, 1992;
172 Tinti and Toniti, 2005; Madsen and Fuhrman, 2008; Madsen and Schaffer, 2010; Antuano and
173 Brocchini, 2008, 2010; Didenkulova, 2009; Dobrokhotoev et al, 2015; Aydin and Kanoglu, 2017).

174 It is worth mentioning that the nonlinear time transformation in (2.11) and (2.12) leads to
175 the shoreline oscillation distortion in comparison with the linear theory predictions. So, for large
176 amplitudes the wave shape becomes multi-valued (broken). The first moment of the wave



177 breaking on the shoreline (the gradient catastrophe) is easily found from (2.12) by calculating the
178 first derivative of the moving shoreline velocity

$$179 \quad \frac{du}{dt} = \frac{dU/dt}{1 - \frac{dU}{dt} / \alpha g}, \quad (2.15)$$

180 from it follows the wave breaking condition

$$181 \quad Br = \frac{\max(dU/dt)}{\alpha g} = \frac{\max(d^2R/dt^2)}{\alpha^2 g} = 1, \quad (2.16)$$

182 where we have introduced the breaking parameter – Br to designate the left-hand side in (2.16),
183 which characterizes the nonlinear wave properties on the shoreline. The condition (2.16) can be
184 given a physical meaning, that the breaking occurs when the last sea particle acceleration ($\alpha^{-1}d^2R/dt^2$)
185 exceeds the component of gravity acceleration along the shoreline ($g\alpha$). As
186 shown in (Didenkulova, 2009), condition (2.16) coincides with (2.10) for Jacobian. It is
187 important to emphasize that the breaking condition is unequivocally found through solving the
188 linear problem of the wave run-up on the shore. It is determined only by the particle acceleration
189 value on the shoreline; but it is not determined separately by the shoreline displacement or its
190 velocity.

191 A similar Carrier – Greenspan transformation is obtained for waves in narrow inclined
192 channels, fjords, and bays (Rybkin et al, 2013; Pedersen, 2016; Anderson et al, 2017; Raz et al,
193 2018); only the wave equation (2.4) and relations (2.5) - (2.8) change. However, the moving
194 shoreline dynamics is still described by equations (2.11) and (2.12), valid for arbitrary cross-
195 section channels.

196

197 **3. The moving shoreline dynamics at an initially monochromatic wave run-up**

198 The monochromatic wave run-up on a flat slope by using the Carrier – Greenspan
199 transformation has been studied in a number of papers cited above. Let us reproduce here the
200 main features of the moving shoreline dynamics necessary for us to draw a statistical description
201 further on. Mathematically, the monochromatic wave run-up is described by an elementary
202 solution of equation (2.4)

$$203 \quad \Phi(\sigma, \lambda) = QJ_0(l\sigma) \cos(l\lambda), \quad (3.1)$$



204 where Q and l are arbitrary constants, and J_0 is the zero-order Bessel function. Far from the
 205 shoreline ($\sigma \rightarrow \infty$) the Bessel function decreases, so the wave function Φ becomes small. In this
 206 case, in (2.5) - (2.8) one can use approximate expressions (the ‘linear’ Carrier – Greenspan
 207 transformation)

$$208 \quad \eta = \frac{1}{2g} \frac{\partial \Phi}{\partial \lambda}, \quad u = \frac{1}{\sigma} \frac{\partial \Phi}{\partial \sigma}, \quad x = -\frac{\sigma^2}{4\alpha g}, \quad t = \frac{\lambda}{\alpha g}, \quad (3.2)$$

209 and using the asymptotic representation for the Bessel function, reduce (3.1) to the expression
 210 for the water surface displacement

$$211 \quad \eta(x, t) = a(x) \left\{ \sin \left[\omega \left(t - \int \frac{dx}{\sqrt{gh(x)}} \right) \right] - \frac{\pi}{4} \right\} + \sin \left[\omega \left(t + \int \frac{dx}{\sqrt{gh(x)}} \right) + \frac{\pi}{4} \right], \quad (3.3)$$

212 where

$$213 \quad a(x) = \frac{Q}{2g} \sqrt{\frac{l}{\pi \sqrt{gh(x)}}}, \quad \omega = gl\alpha. \quad (3.4)$$

214 The wave field away from the shoreline is a superposition of two waves of the same frequency
 215 and a variable amplitude $a(x)$, which together form a standing wave. It immediately shows that
 216 the wave amplitude varies with depth according to the Green law ($h^{-1/4}$), as it should be far from
 217 the coast. The same asymptotic result follows from the exact solution of linear shallow water
 218 equations.

$$219 \quad \eta(x, t) = R_0 J_0 \left(\sqrt{\frac{4\omega^2 |x|}{g\alpha}} \right) \sin(\omega t), \quad (3.5)$$

220 where R_0 is the wave amplitude at the fixed shoreline ($x = 0$), identified with the maximum run-
 221 up height in the linear theory. By connecting (3.4) and (3.5), we obtain the formula for the run-
 222 up height obtained through the incident wave amplitude far from the coast

$$223 \quad \frac{R_0}{a(x)} = \sqrt{\frac{2\omega}{\alpha}} \sqrt{\frac{h(x)}{g}}. \quad (3.6)$$

224 Formula (3.6) allows working further with the run-up height R_0 instead of the wave amplitude far
 225 from the coast $a(x)$, considering it to be given. Having determined Q and l through the incident
 226 wave parameters, we can calculate the run-up characteristics in the nonlinear theory, considering
 227 the limit of formula (3.1) with $\sigma \rightarrow 0$ and using the Carrier – Greenspan transformation formulas
 228 (2.5) - (2.8). The moving shoreline movement is determined by the parametric dependence



$$229 \quad t = \frac{\lambda}{\alpha g} - \frac{\omega R_0}{\alpha^2 g} \cos\left(\frac{\omega \lambda}{\alpha g}\right), \quad (3.7)$$

$$230 \quad r = R_0 \sin\left(\frac{\omega \lambda}{\alpha g}\right) - \frac{\omega^2 R_0^2}{2\alpha^2 g} \cos^2\left(\frac{\omega \lambda}{\alpha g}\right). \quad (3.8)$$

231 It is convenient to introduce dimensionless variables

$$232 \quad z = \frac{r}{R_0}, \quad \tau = \omega t, \quad \varphi = \frac{\omega \lambda}{\alpha g}, \quad (3.9)$$

233 and calculate the breaking parameter

$$234 \quad Br = \frac{\omega^2 R_0}{\alpha^2 g}, \quad (3.10)$$

235 so the formulas (3.7) and (3.8) are finally rewritten in the form

$$236 \quad \tau = \varphi - Br \cos(\varphi), \quad (3.11)$$

$$237 \quad z = \sin(\varphi) - \frac{Br}{2} \cos^2(\varphi), \quad (3.12)$$

238 what is another record for the formulas (2.11) and (2.12), if we take

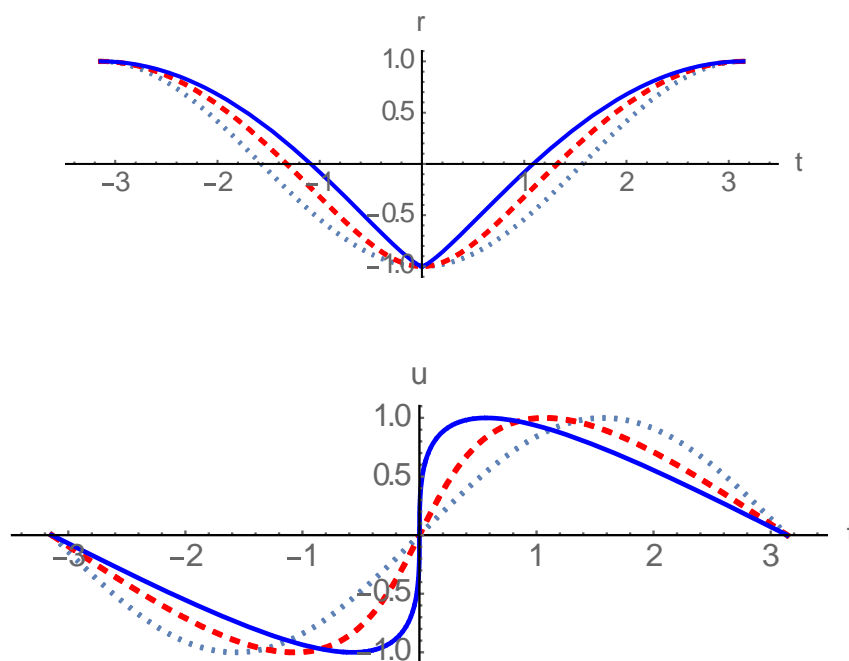
$$239 \quad R(t) = R_0 \sin(\omega t), \quad (3.13)$$

240 arising from (3.5) with $x = 0$. Let us note that the function $z(\tau, Br)$ is set in a parametric form,
 241 but after expressing φ from (3.12) and substituting it in (3.11), we can obtain the explicit
 242 expression for the function $\tau(z; Br)$. In the paper, we will use both explicit and implicit
 243 expressions of the functions describing the moving shoreline dynamics.

244 Fig. 2 shows the moving shoreline dynamics at different wave height values in terms of
 245 the breaking parameter up to the limiting value ($Br = 1$). In the limit of small parameter values,
 246 the oscillations are close to sinusoidal (it is almost a linear problem). Then, with the increasing
 247 amplitude, the moving shoreline velocity gets a steep leading front, while at the moving
 248 shoreline vertical displacement a peculiar feature is formed at the wave run-down stage. As it is
 249 known, at the time of the Riemann wave breaking, a peculiarity like $u \sim t^{1/3}$ is formed
 250 (Pelinovsky et al, 2013). Then, in the integral over the Riemann wave (at the moving shoreline
 251 displacement), this peculiar feature will have the form $z \sim t^{4/3}$. Thus, with the wave amplitude
 252 increase, the first breaking occurs at sea (at the run-down stage), and not on the coast. Then the
 253 breaking zone expands and moves on to the coast, but at this stage, analytical solutions based on
 254 the Carrier-Greenspan transformation become inapplicable.



255
 256



257
 258

259 Fig. 2. The moving shoreline dynamics (top) and its velocity (below) for different breaking
 260 parameter values Br (0 –the dotted line, 0.5 –the dashed line and 1 – the solid line).

261

262 **4. Probabilistic characteristics of the initially sine wave run-up with a random phase**

263 Let us now consider the probabilistic characteristics of the initially sine wave run-up with a
 264 random phase on the shore, assuming it to be uniformly distributed over the interval $[0 - 2\pi]$.
 265 These characteristics are found by using the geometric probability methods (Kendall and Stuart,
 266 1969), so that for ergodic processes the probability density of the moving shoreline vertical
 267 displacement coincides with the relative location time of the function $\xi(t)$ in the interval $(\xi,$
 268 $\xi + d\xi)$

269
$$W(\xi) = \frac{1}{2\pi} \sum_{n=1}^N \left| \frac{dt_n}{d\xi} \right|, \quad (4.1)$$

270 where the summation takes place at all intersection level $\xi(t)$. For harmonic disturbance, it is
 271 enough to restrict ourselves to considering the field on a half-period. So, for the moving
 272 shoreline vertical displacement in dimensionless variables, the derivative $d\tau/dz$ of the



273 parametric curve (3.11) and (3.12) can be calculated through the ratio of the derivatives $d\tau/d\varphi$
 274 и $dz/d\varphi$

$$275 \quad W_z^{\sin}(z; Br) = \frac{1}{\pi} \frac{1 + Br \sin \varphi}{\cos \varphi + Br \cos \varphi \sin \varphi} = \frac{1}{\pi \cos \varphi}, \quad (4.2)$$

276 we indicated here that the probability density depends on Br as a parameter. Finding $\cos \varphi$ from
 277 the formula (3.12) for the vertical displacement, we obtain the final expression for the
 278 probability density

$$279 \quad W_z^{\sin}(z; Br) = \frac{1}{\pi} \frac{1}{\sqrt{1 - \frac{1}{Br^2} \left[1 - \sqrt{1 + 2zBr + Br^2} \right]^2}}, \quad (4.3)$$

280 which in the linear problem for a purely sinusoidal perturbation transforms into a well-known
 281 expression for the probability distribution of a harmonic signal with a random phase (Kendall
 282 and Stuart, 1969)

$$283 \quad W_z^{\sin}(z; 0) = \frac{1}{\pi} \frac{1}{\sqrt{1 - z^2}}. \quad (4.4)$$

284 The probability distribution (4.3) for the three values of the parameter Br is shown in Fig.
 285 3. As you can see, the probability density becomes an asymmetric function with a greater
 286 probability in the area of positive values corresponding to the wave run-up on the coast than at
 287 the run-down stage. At the ends of the interval, the probability density is unlimited throughout
 288 the entire range change of Br , since the shoreline oscillations near the maximum have a zero
 289 derivative (the moving shoreline velocity in it becomes zero).

290 The obtained probability density function can be used to calculate the statistical moments
 291 of the shoreline oscillations. Technically, however, it is easier to use the parametric equations
 292 (3.11) and (3.12) and calculate all the moments.

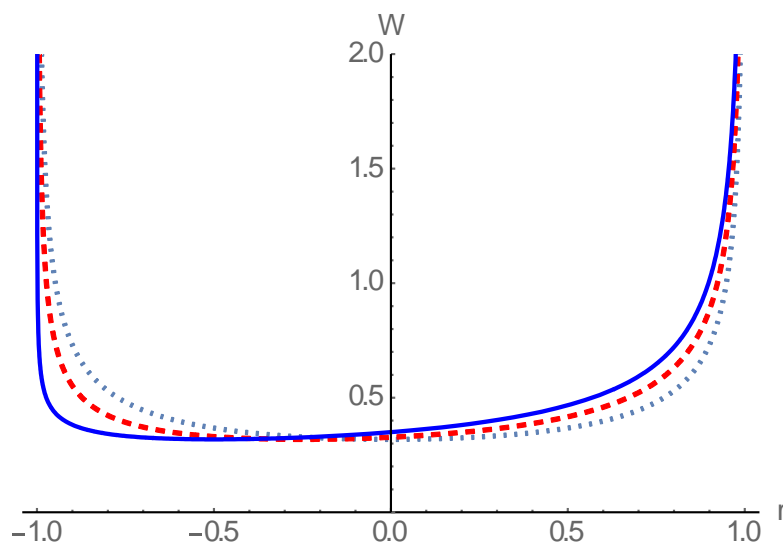
$$293 \quad M_n^z = \frac{1}{2\pi} \int_0^{2\pi} z^n(\tau) d\tau = \frac{1}{2\pi} \int_0^{2\pi} z^n(\varphi) \frac{d\tau}{d\varphi} d\varphi. \quad (4.5)$$

294 So, the first moment

$$295 \quad M_1^z = \frac{Br}{4} \quad (4.6)$$

296 determines the average water level rise on the coast when the waves approach the shore (set-up
 297 phenomenon), which is commonly observed (Dean and Walton, 2009).

298



299

300 Fig. 3. The probability density of the moving shoreline vertical displacement for the initially sine
 301 wave run-up at $Br = 0$ (the dotted line), 0.5 (the dashed line) and 1 (the solid line).

302

303 The second moment determines the dispersion

$$304 \quad \delta^2 = \frac{1}{2\pi} \int_0^{2\pi} (z - M_1^z)^2 d\tau = \frac{1}{2} - \frac{3}{32} Br^2, \quad (4.7)$$

305 characterizing the fluctuation range relative to the average value; it relatively weakly decreases
 306 with the growth of the parameter Br (less than 10% for non-breaking waves).

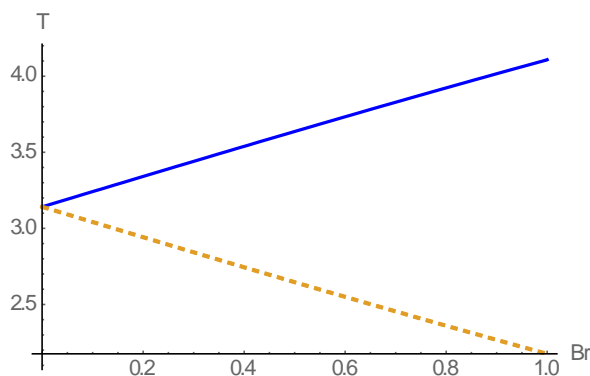
307 Finally, the total flooding time and its drainage time are easy to find from (3.11) and
 308 (3.12), finding from the equation mentioned last, the value φ , at which $z = 0$, and substituting the
 309 obtained values in (3.11)

$$310 \quad T_{flood} = \pi - 2 \arcsin \left[\frac{\sqrt{1 + Br^2} - 1}{Br} \right] + 2\sqrt{2} \sqrt{\sqrt{1 + Br^2} - 1},$$

311 (4.9)

$$312 \quad T_{dry} = \pi + 2 \arcsin \left[\frac{\sqrt{1 + Br^2} - 1}{Br} \right] - 2\sqrt{2} \sqrt{\sqrt{1 + Br^2} - 1},$$

313 Both times change almost linearly with the increasing wave amplitude (parameter Br), see Fig. 4.



314

315 Fig. 4. The total flooding time (the solid curve) and the drainage time (the dashed curve)
 316 depending on the parameter Br .

317

318 It is worth noting that, in contrast to the vertical displacement, the moving shoreline
 319 velocity distribution $[u = (\omega R_0 / \alpha)v]$, as it is easy to show, does not depend on the breaking
 320 parameter and probability density function is determined by the simple formula

321
$$W_v^{\sin}(v) = \frac{1}{\pi} \frac{1}{\sqrt{1-v^2}}. \quad (4.10)$$

322 The distribution independence on the degree of nonlinearity is well known for the Riemann
 323 waves and is explained by the compensation of compression and rarefaction areas (Gurbatov et
 324 al, 1991, 2011).

325

326 **5. Probabilistic characteristics of a narrow-band wave run-up with a random amplitude**
 327 **and phase**

328 Let us consider the run-up of a quasi-harmonic wave with a random amplitude and phase
 329 on a flat slope. To do this, we will first rewrite formulas (4.3) and (4.10) for them to include the
 330 wave amplitude. It is convenient to enter the maximum height R_{max} as the amplitude scales at
 331 which the breaking parameter turns into 1

332
$$Br = \frac{\omega^2 R_{max}}{\alpha^2 g} = 1, \quad (5.1)$$

333 And to use dimensionless displacement ($y=r/R_{max}$). Then the dimensionless amplitude is

334
$$A = \frac{R_0}{R_{max}} \leq 1, \quad (5.2)$$

335 and formula (4.3) is converted to the form $(-A < y < A)$



336
$$W_y^{\sin}(y; A) = \frac{1}{\pi} \frac{1}{\sqrt{A^2 - [1 - \sqrt{1 + 2y + A^2}]^2}} . \quad (5.3)$$

337 Assuming now that the wave amplitude A is a random variable, we average (5.3) by using
338 the amplitude distribution density $W_A(A)$

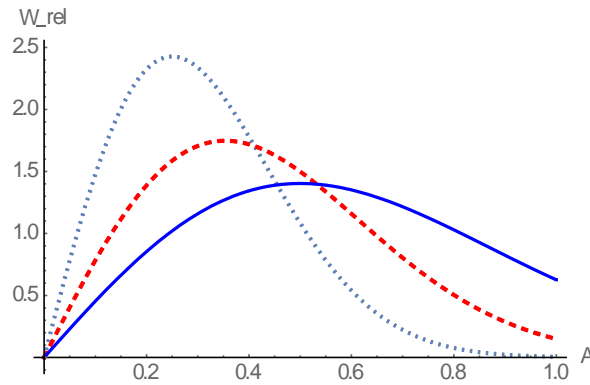
339
$$W(y) = \int_y^\infty W_y^{\sin}(y; A) W_A(A) dA . \quad (5.4)$$

340 Formula (5.4) has an important practical meaning: by the measured distribution of the
341 wave amplitudes far from the coast (re-computed on run-up amplitudes in the linear theory), it is
342 possible to obtain the distribution of the wave run-up characteristics on the coast. The only
343 requirement imposed on the wave ensemble is that it should not contain breaking waves, which
344 should be somehow removed from the record. It immediately follows that the Gaussian field
345 containing large amplitude tails does not fit this requirement, and it should be modified.
346 Therefore, we assume the amplitude distribution to be finite for $A < A_{max} = 1$. In this case, the
347 breaking will not be implemented in any way, and the random wave run-up will take place
348 without any breaking. Further calculations depend on the specific type of the amplitude
349 distribution.

350 Let us construct the finite amplitude distribution at which the linear field distribution is
351 close to the Gaussian form and modify the Rayleigh distribution in the area $A < A_{max} = 1$ (Fig. 5)

352
$$W_A(A; A_{max}, A_s) = \frac{1}{1 - \exp(-2A_{max}^2 / A_s^2)} \frac{4A}{A_s^2} \exp\left(-2\frac{A^2}{A_s^2}\right), A \leq A_{max}, \quad (5.5)$$

353 to make the density function distribution normalized. Here, A_s is the so-called significant wave
354 run-up height (an averaged value of 1/3 highest amplitudes). We would like to note here, that it
355 follows from (2.11) and (2.12) that the extremal run-up characteristics in the nonlinear theory
356 remain the same as in the linear theory. This means that the significant wave run-up height
357 remains the same as in the nonlinear theory.



358

359

360 Fig. 5. The modified Rayleigh distribution (5.5) for different distribution values A_s/A_{max} ;
 361 0.5 –the dotted curve, 0.7 –the dashed line, 1 –the solid line.

362

363 When $A_s \ll A_{max} = I$, distribution (5.5) transforms into the Rayleigh one, which is
 364 characteristic of the Gaussian initial distribution of a narrow-band random signal. With the help
 365 of (5.5), it becomes possible to calculate the distribution function of shoreline oscillations for the
 366 various wave energy. So, with the incident wave small amplitude ($A_s \ll I$), distribution (5.3) can
 367 be replaced by a simpler expression (4.4) and the answer is the run-up distribution characteristics
 368 in the linear theory:

$$369 \quad W_{lin}(y; A_{max}, A_s) = \frac{4}{\pi A_s^2 [1 - \exp(-2A_{max}^2 / A_s^2)]} \int_y^{A_{max}} \frac{A}{\sqrt{A^2 - y^2}} \exp\left(-2\frac{A^2}{A_s^2}\right) dA. \quad (5.6)$$

370 Besides, if $A_s \ll A_{max} = I$, the integral (5.6) is reduced to the Gaussian distribution

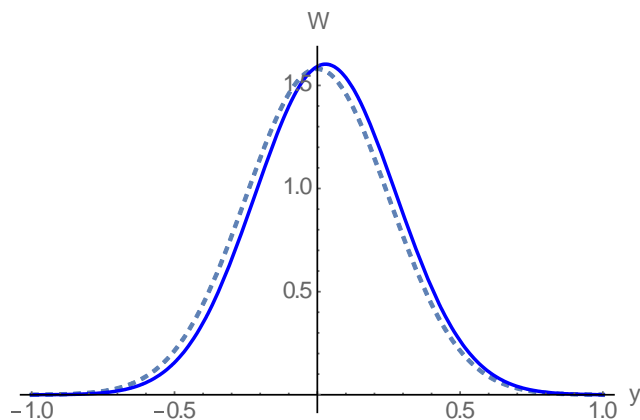
$$371 \quad W_{lin}(y; A_s) = \frac{2}{\sqrt{2\pi} A_s} \exp\left(-2\frac{y^2}{A_s^2}\right), \quad (5.7)$$

372 where, $A_s = 2\sigma_y$, and σ_y^2 is the moving shoreline oscillation dispersion.

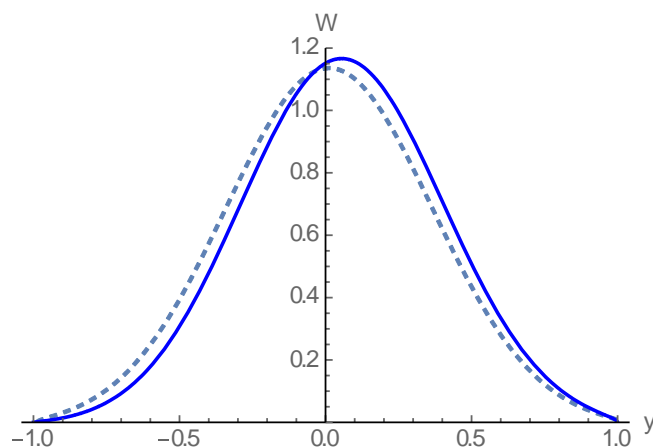
373 Fig. 6 shows the distribution of the run-up characteristics for different ratios of A_s/A_{max}
 374 values by formulas (5.4) and (5.5); they are shown in solid lines. Here the dashed lines show the
 375 calculation results according to the linear theory (5.6). As one can see, with $A_s/A_{max} = 0.5$ (the top
 376 panel) and 0.7 (the middle panel), the linear distribution is close to the Gaussian one.
 377 Nonlinearity leads to the asymmetry of the distribution function density in the direction of
 378 positive values corresponding to the wave characteristics on the coast. If the undisturbed wave
 379 ensemble is made of relatively large waves ($A_s/A_{max} = 1$), their distribution is far from the
 380 Gaussian, both in the linear and in the nonlinear approximation.



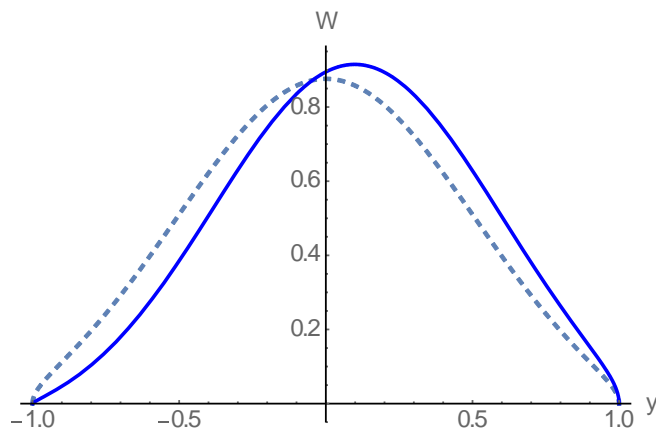
381



382



383



384 Fig. 6. The probabilistic density function of the vertical shoreline displacement in the
385 nonlinear theory (solid lines) and in the linear theory (dashed lines) for different A_s/A_{max} : 0.5
386 values: (the upper panel), 0.7 (the middle panel) and 1 (the lower panel).

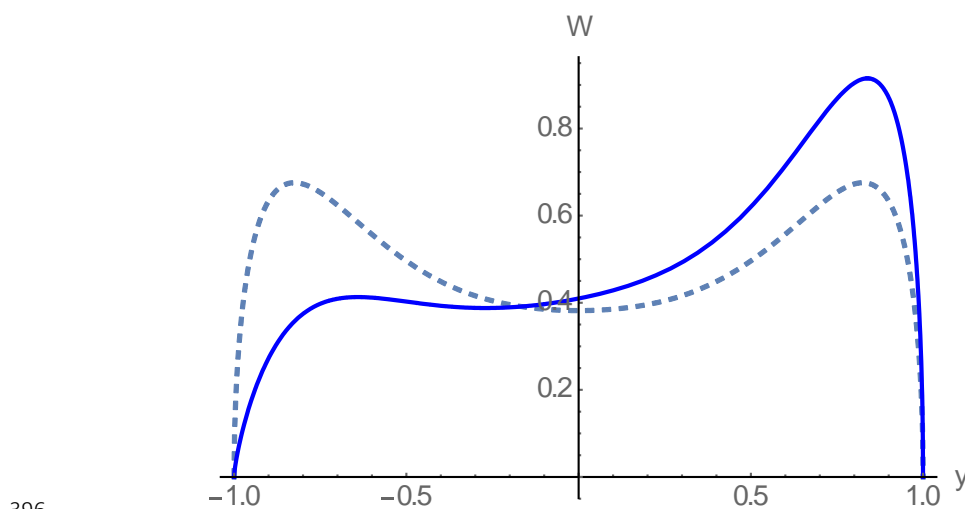
387



388 The finite ($A < A_{max}$) power-law distribution concentrated mainly near the maximum
389 amplitude A_{max} can be considered as another example of undisturbed large-amplitude waves.

390
$$W_A(A) = \frac{6A^5}{A_{max}^6}. \quad (5.8)$$

391 Fig. 7 shows the graphs of the probabilistic density function of the moving shoreline
392 displacement calculated by using formula (5.4) and (4.4) in the linear theory and (5.3) in the
393 nonlinear theory. It is also seen in the figure that nonlinear effects lead to a strong asymmetry
394 towards the positive values, that is, to the wave amplification at the run-up up stage than at the
395 run-down stage.



396
397 Fig. 7. Probabilistic density function of the shoreline vertical displacement in the linear
398 theory (dashed line) and non-linear theory (solid line)

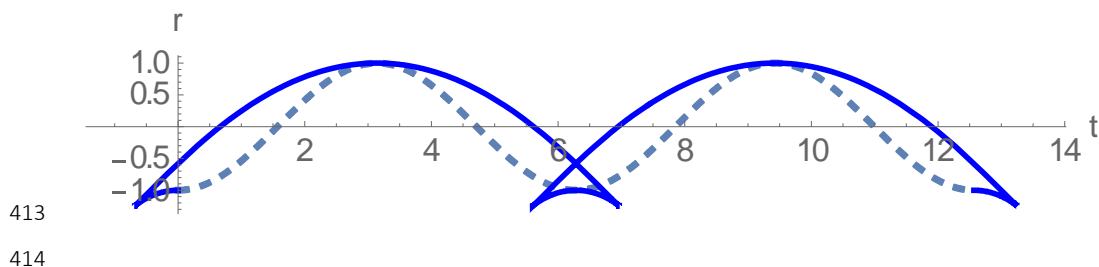
399

400 6. The wave breaking effect on probabilistic run-up characteristics

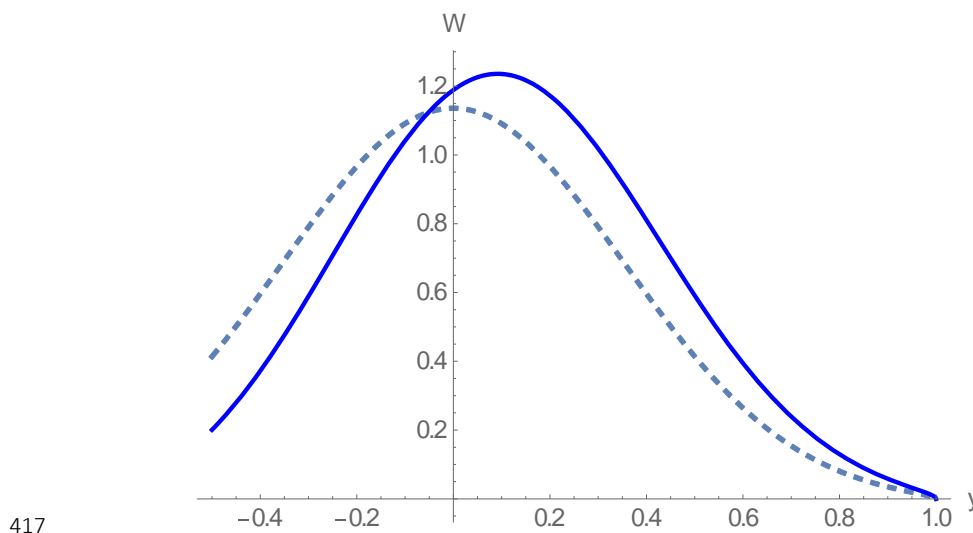
401 The theory described above is valid for non-breaking waves. The mentioned wave ensemble,
402 strictly speaking, cannot be the Gaussian one, as it always has unlimited tails in the probability
403 density function. Let us briefly discuss what the formulas obtained for non-breaking waves lead
404 to in the presence of broken waves. Fig. 8 shows the parametric curve (3.11) - (3.12) when $Br =$
405 2. Formally, the curve became multi-valued in the range of negative values corresponding to the
406 maximum water outflow from the coast. We have already indicated that the probability density
407 function of the moving shoreline vertical displacement $W(\xi)$ coincides with the relative
408 residence time $\xi(t)$ of the function in the interval $(\xi, \xi + d\xi)$, which is calculated by formula



409 (3.1). In contrast to negative cut-off bias values, in the area of positive values there is no
 410 ambiguity, and, therefore, all the calculations can be carried out by using the formulas described
 411 above. An example of such calculation with $Br = 2$ and $r > -0.5$ (in the zone of one-value
 412 solution) is shown in Fig. 9.



413
 414
 415 Fig. 8. The parametric curve (3.11) - (3.12) with $Br = 2$ (the solid curve) in comparison with the
 416 linear problem with $Br = 0$ (the dashed line)



417
 418 Fig. 9. The probability density function at $Br = 2$, constructed by formulas (5.3), (5.4) and (5.5)
 419 (the solid line) in comparison with the linear distribution (5.6) is the dotted line. $A_s/A_{max} = 0.7$.

420
 421 However, these results should be treated with caution, since after the wave breaking at the run-
 422 down stage; it is not obvious that the next wave climbing on the coast will not break. This
 423 important issue requires going beyond the theory discussed in this article.

424
 425
 426



427 **7. Discussion and conclusion**

428 In this paper, we study the run-up of irregular narrow-band waves with a random
429 envelope (swell, storm surges, and tsunami) on a beach of a constant slope. The work was
430 carried out in the framework of the nonlinear wave theory with one important assumption: there
431 should be no breaking waves in the wave ensemble. This restriction is quite strict for field and
432 laboratory conditions, but nevertheless, there are cases when it is performed. For instance, 75%
433 of historical tsunami waves climbed on the coast with no breaking (Mazova et al, 1983). In the
434 experiments performed in the Warwick University tank and in the Large Tank in Hannover
435 (Denissenko et al, 2011, 2013), this condition was fulfilled.

436 The wave nonlinearity at the run-up stage leads to increased deviations from Gaussianity, as
437 might be expected from general considerations. Nevertheless, it is shown that the probability
438 distribution of the moving shoreline velocity does not depend on the wave nonlinearity and can
439 be calculated within the linear theory framework. The same conclusion can be drawn about the
440 distribution of the extreme run-up characteristics (the moving shoreline displacement and speed),
441 which, in fact, has already been discussed earlier (Didenkulova et al, 2008). However, the
442 probabilistic density function of the moving shoreline displacement differs from that predicted
443 one in the linear theory framework. It is described by formula (5.4) by using either the
444 theoretical or the measured distribution of the incident wave amplitudes. The paper gives the
445 calculation results of the probable run-up characteristics with a modified Rayleigh distribution
446 for wave amplitudes.

447 The wave breaking leads to the inapplicability of the wave run-up theory based on the
448 Carrier-Greenspan transformation. If, nevertheless, the share of large amplitude waves is small,
449 the breaking occurs mainly at the run-down stage, having little effect on the long-wave coast
450 flooding characteristics (see Section 6). This question, however, requires a special study based
451 on direct numerical solutions of the shallow-water equations or their nonlinear-dispersive
452 generalizations.

453 Finally, it is worth noting that we considered the narrow-band wave run-up with a
454 random amplitude and phase; as for the random waves with a wide spectrum – it is the problem
455 of further consideration.

456 Obtained probability density functions of the vertical displacement of the moving
457 shoreline are useful to compute statistical characteristics of flooding time and force on coasts and
458 constructions, which are necessary for mitigation of natural marine hazards.



459 **Acknowledgment:**

460 The work is supported by the grants from the Russian Science Foundation: No.19-12-00256 (in
461 part of computing the random Riemann wave characteristics) and No. 19-12-00253 (in part of
462 computations the probability density function of the moving shoreline).

463

464 **References**

465

- 466 1. Anderson, D., Harris, M., Hartle, H., Nicolsky, D., Pelinovsky, E., Raz, A. and Rybkin, A.:
467 Runup of long waves in piecewise sloping U-shaped bays, *Pure and Applied Geophysics*, 174,
468 3185-3207, 2017.
- 469 2. Antuano, M. and Brocchini, M.: Maximum run-up, breaking conditions and dynamical forces
470 in the swash zone: a boundary value approach, *Coastal Engineering*, 55, 732-730, 2008.
- 471 3. Antuano, M. and Brocchini, M.: Solving the nonlinear shallow-water equations in physical
472 space, *J. Fluid Mech.*, 643, 207–232, 2010.
- 473 4. Aydin. B. and Kanoglu, U.: New analytical solution for nonlinear shallow water-wave
474 equations, *Pure and Applied Geophysics*, 174, 3209–3218, 2017.
- 475 5. Bec, J. and Khanin, K.: Burgers turbulence, *Physics Reports*, 447, 1-66, 2007.
- 476 6. Burgers, J. M.: *The Nonlinear Diffusion Equation*. Dordrecht, D. Reidel, 1974.
- 477 7. Carrier, G.F. and Greenspan, H.P.: Water waves of finite amplitude on a sloping beach,
478 *J. Fluid Mech.*, 4, 97–109, 1958.
- 479 8. Choi, J., Kwon, K.K. and Yoon, S.B.: Tsunami inundation simulation of a built-up area using
480 equivalent resistance coefficient, *Coastal Engineering Journal*, 54, 1250015 (25 pages), 2012.
- 481 9. Dean, R.G. and Walton, T.L.: Wave setup. In: Kim, Y.C. (Ed.), *Handbook of Coastal
482 and Ocean Engineering*. World Sci, Singapore, 2009.
- 483 10. Denissenko, P., Didenkulova, I., Pelinovsky, E. and Pearson J.: Influence of the nonlinearity
484 on statistical characteristics of long wave runup, *Nonlinear Processes in Geophysics*, 18, 967-
485 975, 2011.
- 486 11. Denissenko, P., Didenkulova, I., Rodin, A., Listak, M. and Pelinovsky E.: Experimental
487 statistics of long wave runup on a plane beach, *Journal of Coastal Research*, 65, 195-200,
488 2013.
- 489 12. Didenkulova, I.: New trends in the analytical theory of long sea wave runup. In: *Applied
490 Wave Mathematics: Selected Topics in Solids, Fluids, and Mathematical Methods* (Ed: E.
491 Quak and T. Soomere). Springer, 265–296, 2009.
- 492 13. Didenkulova, I., Pelinovsky, E. and Sergeeva, A.: Runup of long irregular waves on plane
493 beach. In: *Extreme Ocean Waves* (Eds: Pelinovsky E., Kharif C.), Springer, 83-94, 2008.



- 494 14.Didenkulova, I.I., Sergeeva, A.V., Pelinovsky, E.N. and Gurbatov, S.N.: Statistical estimates
495 of characteristics of long wave run up on the shore, *Izvestiya, Atmospheric and Oceanic*
496 *Physics*, 46, 530–532, 2010.
- 497 15.Didenkulova, I., Pelinovsky, E. and Sergeeva, A.: Statistical characteristics of long waves
498 nearshore, *Coastal Engineering*, 58, 94-102, 2011.
- 499 16.Dobrokhotov, S.Yu.,Minenkov, D.S., Nazaikinskii, V.E. and Tirozzi, B.: Simple exact and
500 asymptotic solutions of the 1D run-up problem over a slowly varying (quasiplanar) bottom. In
501 *Theory and Applications in Mathematical Physics*, World Scientific, Singapore, 29-47, 2015.
- 502 17.Frisch, U.: *Turbulence: the legacy of A. N. Kolmogorov*, Cambridge University Press, 1995.
- 503 18.Frisch, U. and Bec, J.: Burgulence. In: *New trends in turbulence* (Eds: M. Lesieur, A.Yaglom
504 and F. David), Springer EDP-Sciences, 341–383, 2001.
- 505 19.Gurbatov, S. N., Saichev, A. I. and Shandarin, S. F.: Large-scale structure of the Universe.
506 The Zeldovich approximation and the adhesion model, *Physics Uspekhi*, 55, 223–249, 2012.
- 507 20.Gurbatov, S.N., Malakhov, A.N. and Saichev, A.I.: *Nonlinear Random Waves and*
508 *Turbulence in Nondispersive Media: Waves, Rays, Particles*. Manchester University Press,
509 1991.
- 510 21.Gurbatov, S.N., Rudenko, O.V. and Saichev, A.I.: *Waves and Structures in Nonlinear*
511 *Nondispersive Media*. Berlin, Heidelberg: Springer-Verlag, and Beijing: Higher Education
512 Press, 2011.
- 513 22.Gurbatov, S.N. and Saichev, A.I.: Inertial nonlinearity and chaotic motion of particle fluxes,
514 *Chaos*, 3, 333-358, 1993.
- 515 23.Gurbatov, S., Simdyankin, S., Aurell, E., Frisch, U. and Toth, G.: On the decay of Burgers
516 turbulence, *J. Fluid Mech.*, 344, 349-374, 1997.
- 517 24.Gurbatov, S.N., Deryabin, M.S., Kasyanov, D.A. and Kurin, V.V.: Evolution of narrow-band
518 noise beams for large acoustic Reynolds numbers, *Radiophysics and Quantum Electronics*,
519 61, 478–490, 2018.
- 520 25.Gurbatov, S., Deryabin, M., Kurin, V. and Kasyanov, D.: Evolution of intense narrowband
521 noise beams, *Journal of Sound and Vibration*, 439, 208-218, 2019.
- 522 26.Harris, M.W., Nicolsky, D.J., Pelinovsky, E.N. and Rybkin A.V.: Runup of nonlinear long
523 waves in trapezoidal bays: 1-D analytical theory and 2-D numerical computations, *Pure and*
524 *Applied Geophysics*, 172, 885-899, 2015.
- 525 27.Harris, M.W., Nicolsky, D.J., Pelinovsky, E.N., Pender, J.M. and Rybkin, A.V.: Run-up of
526 nonlinear long waves in U-shaped bays of finite length: Analytical theory and numerical
527 computations, *J Ocean Engineering and Marine Energy*, 2, 113-127, 2016.



- 528 28. Hughes, M.G., Moseley, A.S. and Baldock, T.E.: Probability distributions for wave runup on
529 beaches, *Coastal Engineering*, 57, 575-584, 2010.
- 530 29. Huntley, D.A., Guza, R.T. and Bowen, A.J.: A universal form for shoreline run-up spectra, *J.*
531 *Geophys. Res.*, 82, 2577–2581, 1977.
- 532 30. Kaiser, G., Scheele, L., Kortenhaus, A., Lovholt, F., Romer, H. and Leschka, S.: The
533 influence of land cover roughness on the results of high resolution tsunami inundation
534 modeling, *Nat. Hazards Earth Syst. Sci.*, 11, 2521–2540, 2011.
- 535 31. Kendall, M.G. and Stuart, A.: *The Advanced Theory of Statistics. Volume I. Distribution*
536 *Theory*. London. 1969.
- 537 32. Kian, R., Velioglu, D., Yalciner, A.C. and Zaytsev, A.: Effects of harbor shape on the induced
538 sedimentation; L-type basin, *Journal of Marine Science and Engineering*, 4, 55-65, 2016.
- 539 33. Macabuag, J., Rossetto, T., Ioannou, I., Suppasri, A., Sugawara, D., Adriano, B., Imamura, F.,
540 Eames, I. and Koshimura, S.: A proposed methodology for deriving tsunami fragility functions
541 for buildings using optimum intensity measures, *Nat Hazards*, 84, 1257–1285, 2016.
- 542 34. Madsen, P.A. and Fuhrman, D.R.: Run-up of tsunamis and long waves in terms of surf-
543 similarity, *Coast. Eng.*, 55, 209–223, 2008.
- 544 35. Madsen, P. and Schaffer, H. A.: Analytical solutions for tsunami runup on a plane beach:
545 single waves, N-waves and transient waves, *J. Fluid Mech.*, 645, 27-57, 2010.
- 546 36. Mazova, R.Kh., Pelinovsky, E.N. and Solov'yev, S.L.: Statistical data on the tsunami runup
547 onto shore, *Oceanology*, 23, 698 – 702, 1983.
- 548 37. Molchanov, S.A., Surgailis, D. and Woyczynski, W.A.: Hyperbolic asymptotics in Burgers'
549 turbulence and extremal processes, *Comm. Math. Phys.*, 168, 209-226, 1995.
- 550 38. Ozer, S.C., Yalciner, A.C. and Zaytsev, A.: Investigation of tsunami hydrodynamic
551 parameters in inundation zones with different structural layouts, *Pure and Applied*
552 *Geophysics*, 172, 931–952, 2015a.
- 553 39. Ozer, S.C., Yalciner, A.C., Zaytsev, A., Suppasri, A. and Imamura, F.: Investigation of
554 hydrodynamic parameters and the effects of breakwaters during the 2011 Great East Japan
555 Tsunami in Kamaishi Bay, *Pure and Applied Geophysics*, 172, 3473–3491, 2015b.
- 556 40. Park, H., Cox, D.T. and Barbosa, A.R.: Comparison of inundation depth and momentum flux
557 based fragilities for probabilistic tsunami damage assessment and uncertainty analysis,
558 *Coastal Eng.*, 122, 10–26, 2017.
- 559 41. Pelinovsky, E. and Mazova, R.: Exact analytical solutions of nonlinear problems of tsunami
560 wave run-up on slopes with different profiles, *Nat. Hazards*, 6, 227–249, 1992.



- 561 42.Pelinovsky, D., Pelinovsky, E., Kartashova, E., Talipova, T. and Giniyatullin, A.: Universal
562 power law for the energy spectrum of breaking Riemann waves, *JETP Letters*, 98, 237-241,
563 2013.
- 564 43.Pedersen, G.: Fully nonlinear Boussinesq equations for long wave propagation and run-up in
565 sloping channels with parabolic cross sections, *Natural Hazards*, 84, S599–S619, 2016.
- 566 44.Qi, Z.X, Eames, I. and Johnson E.R.: Force acting on a square cylinder fixed in a free-surface
567 channel flow, *J Fluid Mech*, 756, 716–727, 2014.
- 568 45.Raz, A., Nicolisky, D., Rybkin, A. and Pelinovsky, E.: Long wave run-up in asymmetric bays
569 and in fjords with two separate heads, *Journal of Geophysical Research – Oceanus*, 123,
570 2066-2080, 2018.
- 571 46.Rudenko, O.V. and Soluyan S.I.: *Nonlinear Acoustics*. Pergamon Press, NY, 1977.
- 572 47.Rybkin, A. Pelinovsky, E.N. and Didenkulova, I.: Nonlinear wave run-up in bays of arbitrary
573 cross-section: generalization of the Carrier-Greenspan approach, *J Fluid Mechanics*, 748, 416-
574 432, 2014.
- 575 48.Shimozono, T.: Long wave propagation and run-up in converging bays, *J. Fluid Mech.*, 798,
576 457-484, 2016.
- 577 49.Synolakis, C.E.: The runup of solitary waves, *J. Fluid Mech.*, 185, 523–545, 1987.
- 578 50.Synolakis, C., Bernard, E.N., Titov, V.V., Kanoglu, U. and Gonzalez, F.I.: Validation and
579 verification of tsunami numerical models, *Pure and Applied Geophysics*, 165, 2197-2228,
580 2008.
- 581 51.Tinti, S. and Tonini, R.: Analytical evolution of tsunamis induced by near-shore earthquakes
582 on a constant-slope ocean, *J. Fluid Mech.*, 535, 33–64, 2005.
- 583 52.Woyczynski, W.A.: *Burgers–KPZ Turbulence*. Gottingen Lectures, Berlin, Springer-Verlag,
584 1998.
- 585 53.Xiong, Y., Liang, Q., Park, H., Cox, D. and Wang, G.: A deterministic approach for assessing
586 tsunami-induced building damage through quantification of hydrodynamic forces, *Coastal*
587 *Engineering*, 144, 1-14, 2019.
- 588
589
590
591
592
593
594
595
596